Available at www.sciencedirect.com

Metabolism

www.metabolismjournal.com

Effects of vitamin K on the morphometric and material properties of bone in the tibiae of growing rats

*Takeshi Matsumoto**, *Takushi Miyakawa*, *Daiki Yamamoto*

Bioengineering Division, Osaka University Graduate School of Engineering Science, Machikaneyama-cho 1-3, Toyonaka 560-8531, Japan

ARTICLE INFO

Article history:
Received 7 May 2011
Accepted 28 July 2011

ABSTRACT

Suboptimal vitamin K nutriture is evident during rapid growth. We aimed to determine whether vitamin K_2 (menaquinone-4 [MK-4]) supplementation is beneficial to bone structure and intrinsic bone tissue properties in growing rats. Male Wistar rats (5 weeks old) were assigned to either a control diet (n = 8) or an MK-4–supplemented diet (22 mg d^{-1} kg^{-1} body weight, n = 8). After a 9-week feeding period, we determined the serum concentration ratio of undercarboxylated osteocalcin to γ-carboxylated osteocalcin and the urinary deoxypyridinoline level. All rats were then euthanized, and their tibiae were analyzed by micro–computed tomography for trabecular architecture and synchrotron radiation micro–computed tomography for cortical pore structure and mineralization. Fourier transform infrared microspectroscopy and a nanoindentation test were performed on the cortical midlayers of the anterior and posterior cortices to assess bone tissue properties. Neither body weight nor tibia length differed significantly between the 2 groups. Dietary MK-4 supplementation decreased the ratio of undercarboxylated osteocalcin to γ-carboxylated osteocalcin but did not affect deoxypyridinoline, indicating a positive effect on bone formation but not bone resorption. Trabecular volume fraction and thickness were increased by MK-4 ($P < .05$). Neither the cortical pore structure nor mineralization was affected by MK-4. On the other hand, MK-4 increased mineral crystallinity, collagen maturity, and hardness in both the anterior and posterior cortices ($P < .05$). These data indicate the potential benefit of MK-4 supplementation during growth in terms of enhancing bone quality.

1. Introduction

The growth spurt period is crucial for skeletal development; however, bone is vulnerable to fracture during this period because the maintenance of bone strength fails to keep up with the rapid bone extension [1]. Indeed, fracture incidence during this period peaks around the age of peak height velocity [2]. Meanwhile, limb fracture incidence increases among children and adolescents at specific sites [3]; but the mechanisms responsible for this increase have not been identified. Fractures during this period lead to a decrease in the bone mass achieved by the end of adolescence [4]. Furthermore, there is growing evidence that peak bone mass affects the consequences of age-related or postmenopausal bone loss on fracture risk [5,6] and that a lower peak bone density hastens the onset of osteoporosis [7]. Therefore,

Author contributions: T. Matsumoto defined the research theme, carried out the synchrotron radiation micro–computed tomography, interpreted the test results, and wrote the paper. T. Miyakawa carried out the Fourier transform infrared microspectroscopy and nanoindentation test. D. Yamamoto carried out the laboratory micro–computed tomography. All authors designed the methods and experiments, and have contributed to, read, and approved the manuscript.

* *Corresponding author*. Tel.: +81 6 6850 6181; fax: +81 6 6850 6212.
E-mail address: matsu@me.es.osaka-u.ac.jp (T. Matsumoto).

0026-0495/$ – see front matter © 2012 Elsevier Inc. All rights reserved.
doi:10.1016/j.metabol.2011.07.018

fractures during growth spurts not only are detrimental to healthy bone development but also pose the potential risk of osteoporosis later in life [8].

One strategy to prevent fractures during growth and possibly contribute to reducing osteoporotic fracture risk later in life is to increase bone strength. Bone strength is influenced by physical activity and nutritional status. Among the nutritional factors, vitamin K is positively associated with childhood bone mineral acquisition [9]. There are 2 important forms of vitamin K: phylloquinones (vitamin K_1 series, synthesized by green plants) and menaquinones (vitamin K_2 series, synthesized by intestinal bacteria). Vitamin K acts as a cofactor in the posttranslational γ-carboxylation of osteocalcin (OC), the most abundant noncollagenous bone matrix protein synthesized by osteoblasts. In this carboxylation process, glutamate residues are converted into γ-carboxyglutamate, thereby enabling OC to bind to hydroxyapatite and contribute to the structural integrity of bone [10]. Furthermore, vitamin K directly activates steroid and xenobiotic receptors in osteoblastic or preosteoblastic cells to promote collagen accumulation and osteoblast differentiation [11,12] and exerts an antiresorptive action on bone [13].

The concentration ratio of undercarboxylated OC (Glu-OC) to γ-carboxylated OC (Gla-OC), a reliable and stable marker of the vitamin K status of bone, is markedly higher in children than in adults [14]. The elevation of this ratio (Glu/Gla-OC) indicates a suboptimal vitamin K status of bone [15], which is probably a result of high bone metabolic activity during growth [16,17]. Thus, the supplemental intake of vitamin K during childhood and adolescence may be beneficial for healthy bone growth and fracture risk reduction. However, vitamin K's effect on bone structure and intrinsic bone tissue properties has not been entirely explored.

This study was undertaken to test the hypothesis that supplementation with vitamin K is beneficial for enhancing bone quality during growth. For this purpose, we comprehensively compared bone quality (ie, the material and morphological properties of bone) between tibiae of growing rats with and without dietary intake of menaquinone-4 (MK-4), which is endogenously converted from phylloquinones and is predominantly found in tissues [18]. We used Fourier transform infrared microspectroscopy (FTIR-MS) [19,20] and a nanoindentation test [21,22] for measuring the intrinsic properties of the cortical bone tissue, laboratory micro–computed tomography (μCT) for imaging the trabecular architecture [23], and synchrotron radiation μCT (SRμCT) [24,25] for high-resolution imaging of the cortical pore structure and degree of mineralization.

2. Methods

2.1. Animals and diets

Experiments were conducted in accordance with the guiding principles of the American Physiological Society and with the approval of the Animal Research Committee of Osaka University Graduate School of Engineering Science. Male Wistar rats aged 4 weeks (n = 16) and purchased from CLEA Japan (Tokyo, Japan) were housed 2 per plastic cage under controlled conditions (12-hour light/dark cycle, 25°C, 60% humidity) and were allowed free access to a standard diet (CE-2: 1.18% Ca, 1.03% inorganic phosphorus, 0.29% Mg, 2.0 IU/g vitamin D_3; CLEA Japan) and tap water. After a 1-week adaptation period, rats were divided into 2 diet groups: the control diet group (C, n = 8), continuously fed the standard diet, and the MK-4 diet group (M, n = 8), fed the same diet supplemented with MK-4 (350 mg/kg diet; Eisai, Tokyo, Japan). Dietary intake and body weight were measured once a week, and the animals were euthanized by an overdose of pentobarbital sodium at the age of 14 weeks.

2.2. Bone markers

On the day before euthanization, the rats were loaded with 1 mL of distilled water per 100 g of body weight intraperitoneally; and overnight (12 hours) urine samples were collected under fasting conditions in individual metabolic cages. On the day of euthanization, following anesthetization with pentobarbital sodium (50 mg/kg body weight, intraperitoneally), blood samples were collected from the femoral vein and centrifuged at 1000*g* for 10 minutes to separate serum. Serum and urine were stored at −30°C until assaying. Urinary deoxypyridinoline (Dpy) level and serum levels of Gla-OC and Glu-OC were measured by competitive enzyme immunoassay using a Dpy kit (Osteolinks DPD; Sumitomo Pharmaceuticals, Osaka, Japan) and Gla-OC and Glu-OC test kits (MK121 and MK122; Takara Bio, Shiga, Japan), respectively, according to the manufacturers' instructions. To determine the intra- and interassay variations, all samples were assayed in triplicate for each marker; and triplicate measurements were made on 3 consecutive days.

2.3. Sample preparation

The right tibia was harvested from the rats and dissected free of soft tissue. Tibial length (from the proximal-most portion of the convexity of the tibial condyles to the concavity of the distal articular surface of the tibia) and weight were measured with an electronic caliper and balance, respectively. The bone was then transected using a low-speed diamond wheel saw (SBT650; South Bay Technology, San Clemente, CA) at 4 points: 4 mm distal to the proximal tibial growth plate and 11, 6, and 1 mm proximal to the tibiofibular junction. The proximal epimetaphyseal and distal diaphyseal specimens were soaked in 70% ethanol for μCT scanning, and the mid-diaphyseal specimen was wrapped with moistened saline gauze and stored at −30°C for FTIR-MS and the nanoindentation test (Fig. 1).

2.4. Structural analysis by μCT

The proximal metaphysis and distal diaphysis were scanned to image the trabecular architecture and cortical porous network using a μCT system (SMX-1000/VCT; Shimadzu, Kyoto, Japan) and an SRμCT system available at BL20B2 in SPring-8 (Harima, Japan), respectively. The scanning parameters for the laboratory μCT were as follows: 90 keV, 110 μA, 600-millisecond integration time, and 600 projections over 360°. In the SRμCT, a 20-keV monochromatic light (>1 × 10^9 photons/s·mm^2) was used with scanning parameters of an

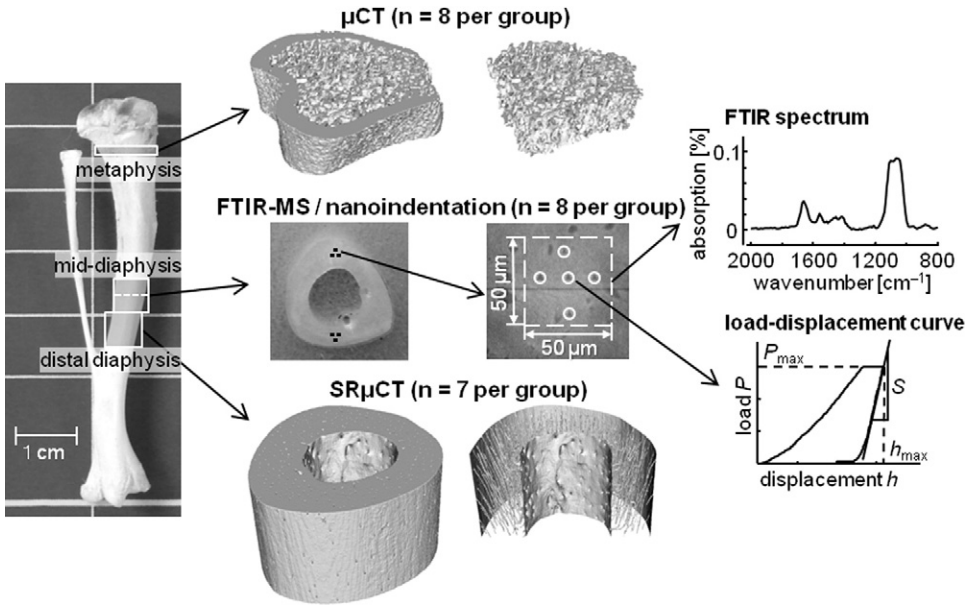

Fig. 1 – Diagram of bone segments measured for each analysis: metaphysis for laboratory μCT, distal diaphysis for SRμCT, and mid-diaphysis for FTIR-MS and nanoindentation. The indentation test included 5 indents in each of 3 anterior and 3 posterior regions where FTIR spectra were obtained.

800-millisecond view exposure time and 900 projections over 180°. The detailed experimental arrangement for using a monochromatic SR beam has been described elsewhere [26]. Image reconstruction was carried out for a 1.2-mm–long section of the cancellous-rich metaphysis 1.0 mm distal to the growth plate (12-μm cubic voxel) and 2.5-mm–long midportion of the diaphysis (2.74-μm cubic voxel), both with an 8-bit grayscale resolution. Using K_2HPO_4 phantom solutions at various concentrations (0.36-1.29 g/cm^3), the relation $\mu_{bone} = 5.50 \cdot \rho_{bone} + 0.87$ ($r^2 > 0.999$) was obtained in SRμCT images, where μ_{bone} (cm^{-1}) is a voxel value of the linear absorption coefficient and ρ_{bone} (g/cm^3) is mineral density. Two specimens, one each from M and C, could not be scanned by SRμCT because of the limited time allocated for the use of an SR beam.

Metaphyseal μCT images were binarized to separate pure bone from the background by the method of Otsu [27]. The outer and inner borders of the cortical bone were determined by raster scanning in multiple directions after filling all bone pores, and the trabecular and cortical compartments were segmented for structural analysis. Diaphyseal SRμCT images showed cortical bone only, which could be extracted distinctly by setting a global threshold of $\rho_{bone} = 0.8$ g/cm^3.

For metaphyseal bone analysis, the following structural indices were determined: cortical bone volume (Cor.V, mm^3), medullary tissue volume (TV, mm^3), fraction of trabecular bone volume (BV/TV, %), trabecular thickness (Tb.Th, μm), trabecular number (Tb.N, mm^{-1}), trabecular separation (Tb.Sp, μm), and trabecular connectivity density (Tb.Conn.D, mm^{-3}). A 3-dimensional method [28] was used for computing Tb.Th, Tb.N, and Tb.Sp. For diaphyseal bone analysis, the following structural indices were determined: Cor.V, TV, cortical porosity (Po, %), mean canal diameter (Ca.Dia, μm), canal density in the endocortical (inner cortical) surface (E.Ca.D, mm^{-2}), canal density in the periosteal (outer cortical) surface (P.Ca.D, mm^{-2}), and density of the intracortical canal connections (Ca.Conn.D, mm^{-3}). Here, enclosed pores within the bone and dead-end pores on the bone surfaces or cross sections of the measured regions were calculated in Po but not in Ca.dia, E.Ca.D, P.Ca.D, or Ca.Conn.D. Canal diameter was determined as the diameter of the largest circle included in the canal cross section, and Ca.Dia was defined as the average of all pore diameters measured in all cross sections. To reflect the highest degree of connectivity in Tb.Conn.D and Ca.Conn.D, 26-adjacency was adopted. The mean ρ_{bone} of diaphyseal cortical bone, dBM (g/cm^3), was also determined by the μ_{bone}-ρ_{bone} relation.

2.5. *Fourier transform infrared microspectroscopy*

The mid-diaphyseal specimens were slowly thawed and embedded in polymethylmethacrylate without ethanol fixation to avoid the possible deterioration of collagen [29]. After polymerization, the position showing the midsection of a specimen was marked on each polymethylmethacrylate block surface. Afterward, using silicon carbide abrasive paper of decreasing particle size (600, 800, and 1200 grit), the proximal surface of an embedded specimen was sanded perpendicularly to the tibial long axis in deionized water until the midlength mark was reached. Finally, the surface was polished with 0.05-μm alumina suspension (AP-D; Struers, Ballerup, Denmark) to a state close to a mirror surface [30]. The proximal cross section was ultrasonically cleaned to remove surface debris and heated at 50°C for 24 hours in ambient air to prevent the enzymatic degradation of collagen [29]. Each cortical cross section was analyzed for chemicals using an FTIR-MS system (IRPrestige-21/AIM-8800; Shimadzu) in the reflection mode. Spectra were collected from three 50 × 50–μm^2 regions each at the anterior and posterior cortical midlayers (Fig. 1) under the conditions of 4 cm^{-1} spectral resolution and 50 scans per point.

The obtained data were corrected for background and converted to absorbance units by the Kramers-Kronig transformation. The following chemical indices were determined: (1) mineral-to-matrix ratio, estimated as the integrated area ratio of the phosphate band (1200-930 cm^{-1}; baseline, 1200-930 cm^{-1}) to the amide I band (1720-1600 cm^{-1}; baseline, 1720-1600 cm^{-1}); (2) mineral crystallinity (the ratio of apatitic to nonapatitic phosphate), estimated by the peak height ratio of 1030/1020 cm^{-1} (baseline, 1200-930 cm^{-1}); and (3) collagen maturity (the ratio of nonreducible to reducible collagen cross-links), estimated by the peak height ratio of 1660/1690 cm^{-1} (baseline, 1720-1600 cm^{-1}). To resolve overlapping bands, the spectra were processed using PEAKFIT software (SeaSolve, San Jose, CA). Second-derivative spectra, accompanied by 9-data-point Savitsky-Golay smoothing, were calculated to identify the positions of the component bands in the spectra. These wavenumbers, which are in close agreement with published data [31,32], were used for curve fitting with Gaussian component peaks. The position, half-bandwidth, and amplitude of the peaks were altered until the resulting bands shifted by no more than 3 cm^{-1} from the initial parameters and good agreements between the calculated sum of all components and the experimental spectra were achieved ($r^2 > 0.999$).

2.6. Nanoindentation test

After FTIR-MS, the specimens were subjected to the nanoindentation test using a dynamic ultra-micro-hardness tester (DUH-201S; Shimadzu) equipped with a diamond Berkovich tip (tip curvature radius <100 nm). Five points were placed near the center and 4 corners of each region where the chemical data were collected, and they were tested with a trapezoidal loading waveform (loading-holding-unloading, Fig. 1): a maximum load of 6000 μN with a loading/unloading rate of 300 μN/s, resulting in a time to peak force of 20 seconds and a 100-second holding period at the maximum load [33]. Mechanical indices were calculated from a resulting force-displacement (P-h) curve according to Oliver and Pharr [34].

The indentation modulus, in combination with the local elastic modulus $E_{specimen}$ and the Poisson ratio $\nu_{specimen}$ of the specimen, is given by the following formula:

$$\text{Indentation modulus} = \frac{E_{specimen}}{1-\upsilon^2_{specimen}} = \left(\frac{1}{E_r} - \frac{1-\upsilon^2_{tip}}{E_{tip}}\right)^{-1}, \quad (1)$$

where E_{tip} (1131 GPa) and ν_{tip} (0.07) are the elastic modulus and Poisson ratio of the diamond indenter, respectively, and E_r is the reduced modulus. The latter was derived from the slope S at the point of initial unloading ($h = h_{max}$) and the contact area A_c, which have a direct relationship with E_r:

$$S(h_{max}) = \left.\frac{dP}{dh}\right|_{h=h_{max}} = \frac{2}{\sqrt{\pi}} E_r \sqrt{A_c}. \quad (2)$$

The ratio of maximum force P_{max} (P at $h = h_{max}$) to A_c gives hardness, interpreted as a measure of strength, which is specifically resistance to nonelastic deformation under pressure:

$$\text{Hardness} = \frac{P_{max}}{A_c}. \quad (3)$$

2.7. Statistics

Differences in the bone markers, bone structural indices, and dBM between M and C were assessed by an unpaired t test. Chemical and mechanical indices determined by FTIR-MS and the nanoindentation test were averaged over 3 regions and 15 indents, respectively, each at the anterior and posterior cortical midlayer sites, and were subsequently analyzed to examine the interaction effect between MK-4 and anatomical site by 2-way repeated-measure analysis of variance. Because no significant interactions between MK-4 and cortical site or any site-specific differences were found in the chemical and mechanical indices, all data measured at 6 regions in the FTIR-MS and 30 indents in the nanoindentation test were pooled for each specimen; and differences in mean values between M and C were analyzed by an unpaired t test. When variances were significantly different according to the F test, an unpaired t test with Welch correction was used. Data are expressed as the mean (standard deviation) values, unless otherwise noted. All data were analyzed by Prism 4 (version 4.0c; GraphPad Software, San Diego, CA) and R (version 2.12.0; R Project for Statistical Computing, Vienna, Austria), and $P < .05$ was considered statistically significant.

3. Results

The actual MK-4 intake in M was 22 mg d^{-1} kg^{-1} body weight, as calculated from average diet intake and body weight. Body weights increased in 9 weeks by 67% (8%) and 71% (8%) in M and C, respectively, and did not differ between M and C at the age of either 5 or 14 weeks (Table 1). No significant differences were found between M and C in tibial weight or length at the age of 14 weeks.

Neither Gla-OC nor Glu-OC differed between M and C. However, Glu/Gla-OC was significantly lower in M than in C (Table 1); and the ratio of Glu-OC to total OC (Gla-OC + Glu-OC) was also significantly lower in M (0.40 [0.06] vs 0.48 [0.03]). No effect of MK-4 was found on bone resorption activity, as indicated by the lack of any difference in urinary Dpy level between M and C. The mean (range) of the intraassay coefficient of variation was 5.8% (2.4%-8.8%) for Dpy, 7.4% (6.7%-8.4%) for Gla-OC, and 7.8% (6.5%-9.7%) for Glu-OC; the mean (range) of the interassay coefficient of variation was

Table 1 – Effects of MK-4 on growth and bone metabolism

	M	C
Body weight, 5 wk (g)	127 (6)	119 (9)
Body weight, 14 wk (g)	212 (13)	203 (14)
Tibial weight (g)	0.50 (0.02)	0.50 (0.03)
Tibial length (mm)	35.6 (0.5)	35.5 (0.5)
Gla-OC (ng/mL)	279 (39)	262 (28)
Glu-OC (ng/mL)	190 (48)	240 (16)
Glu/Gla-OC	0.68 (0.15) *	0.93 (0.11)
Dpy (nmol/mmol Cr)	170 (18)	169 (39)

Data are the mean (SD); n = 8 per group.
* $P < .05$ vs C; unpaired t test.

5.2% (4.3%-6.1%) for Dpy, 4.4% (2.7%-5.7%) for Gla-OC, and 3.2% (1.9%-4.5%) for Glu-OC.

The structural data of the trabecular and cortical bones are summarized in Table 2. At the proximal metaphysis, MK-4 had no effect on either Cor.V or TV; but it increased BV/TV with increasing Tb.Th and decreasing Tb.Sp. At the distal diaphysis, no effect of MK-4 was found on Po or the other indices of intracortical canal structure, including Cor.V and TV.

The chemical compositions and mechanical properties in the mid-diaphyseal bone are summarized in Table 3. There was no effect of MK-4 on the dBM or mineral-to-matrix ratio, but MK-4 increased both mineral crystallinity and collagen maturity. An increasing effect of MK-4 was also found on bone hardness but not on the indentation modulus. Fig. 2 shows the plots of the mineral crystallinity, collagen maturity, and hardness for each specimen. No correlation was found between any of the chemical compositions and mechanical properties in any group or in the pooled data of M and C.

4. Discussion

Although vitamin K supplementation in healthy children enhances the γ-carboxylation of OC [14] and may contribute to bone mineral acquisition [9], there is a lack of experimental data on this issue. To the best of our knowledge, this is the first comprehensive experimental study of the effects of MK-4 on bone quality during growth. We found that, in the growing rat tibia, MK-4 supplementation enhanced trabecular bone structure and increased mineral crystallinity, collagen maturity, and hardness of cortical bone tissue, leading to better bone quality.

The present MK-4 supplementation enhanced the γ-carboxylation of OC, as indicated by a lower Glu/Gla-OC in M than in C, and increased cancellous bone volume, mainly through trabecular bone thickening. The lack of any difference in urinary Dpy excretion between M and C implies that the effectiveness of MK-4 on trabecular bone results from its beneficial function in bone formation rather than its antiresorptive action. A similar effect of daily MK-4 intake (30 mg/kg body weight) has also been observed in the tibial metaphyses of growing rats [35], although the short MK-4 administration period of 5 weeks seemed insufficient for inducing significant changes.

Table 2 – Effects of MK-4 on bone architecture

	M	C
Metaphysis		
Cor.V (mm^3)	5.0 (0.2)	5.0 (0.3)
TV (mm^3)	7.8 (1.0)	7.6 (0.6)
BV/TV (%)	18.5 (3.3)*	14.9 (2.5)
Tb.Th (μm)	50.3 (2.0)*	48.1 (1.9)
Tb.N (mm^{-1})	8.3 (0.4)	7.9 (0.5)
Tb.Sp (μm)	69.8 (6.9)*	79.0 (8.2)
Tb.Conn.D (mm^{-3})	622 (186)	588 (126)
Diaphysis		
Cor.V (mm^3)	9.3 (0.3)	9.5 (0.8)
TV (mm^3)	2.9 (0.2)	3.2 (0.3)
Po (%)	1.2 (0.2)	1.2 (0.2)
Ca.Dia (μm)	12.0 (0.6)	12.2 (0.6)
E.Ca.D (mm^{-2})	25 (6)	30 (4)
P.Ca.D (mm^{-2})	14 (3)	14 (2)
Ca.Conn.D (mm^{-3})	37 (13)	28 (4)

Data are the mean (SD); n = 8 per group for metaphyseal analysis and n = 7 per group for diaphyseal analysis.
* $P < .05$ vs C; unpaired *t* test.

Table 3 – Effects of MK-4 on the chemical and mechanical properties of cortical bone

	M	C
dBM (g/cm^3)	1.24 (0.02)	1.23 (0.01)
Mineral-to-matrix ratio	9.3 (0.7)	9.3 (1.1)
Mineral crystallinity	1.7 (0.3)*	1.5 (0.2)
Collagen maturity	3.2 (0.6)*	2.5 (0.7)
Indentation modulus (GPa)	27.5 (5.3)	26.6 (4.8)
Hardness (GPa)	1.6 (0.4)*	1.3 (0.2)

Data are the mean (SD); n = 8 per group except for dBM (n = 7).
* $P < .05$ vs C; unpaired *t* test.

The antiresorptive or therapeutic action of MK-4 in trabecular and cortical bone structure is well established in rat models of bone disease [36-38]; however, the effect of MK-4 on bone structure during growth has been less explored. The present study showed that MK-4 supplementation did not affect trabecular network connectivity but increased trabecular bone volume and thickness, indicating the benefit of MK-4 supplementation on cancellous bone strength. Because the development of the collagen network precedes the progress of skeletal calcification, the formation of a collagen matrix in the trabeculae will also be promoted by MK-4. On the other hand, no effect of MK-4 was found in cortical bone structure. A different activity of bone modeling/remodeling may be involved in the different effects of MK-4 in trabecular and cortical bone. Changes in bone mass in rats likely occur in trabecular bone–rich regions and less so in cortical bone–rich regions, and the metabolic turnover for trabecular bone is faster than that for cortical bone [39]. Furthermore, the formation of the cortical bone microstructure is strongly coupled to intracortical vascularization, thereby facilitating the bone blood supply required for rapid bone growth [40]. Given these situations, it is possible that the effect of MK-4 on bone structure during growth differs between trabecular and cortical bone.

The present MK-4 supplementation is also unlikely to affect cortical mineralization and collagen concentration because neither the dBM nor mineral-to-matrix ratio differed between M and C. However, the mineral crystallinity and collagen maturity were higher in M than in C. In the present study, mineral crystallinity reflected mineral maturity rather than crystal size or crystalline perfection because it was determined as the ratio of apatitic to nonapatitic phosphate. Thus, it can be assumed that MK-4 contributes to the maturation of cortical bone tissue. Crystal size or crystalline perfection generally evolves in parallel with mineral maturity but reaches completion more slowly [41].

Cortical bone hardness was higher in M than in C, but no difference was found in the indentation modulus between the 2 groups. These results are consistent with an earlier study [30] that showed a positive correlation between hardness and

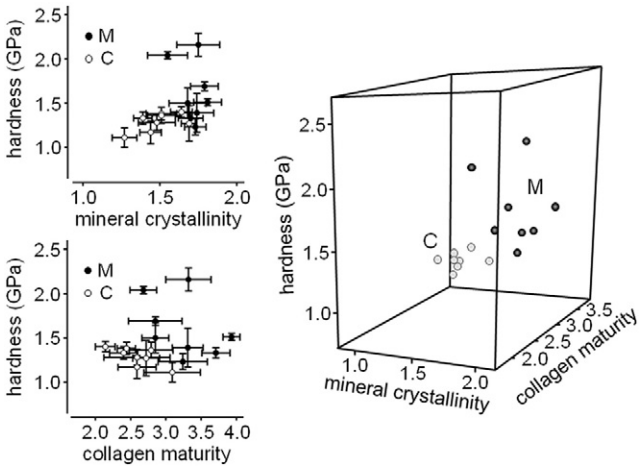

Fig. 2 – Left: plots of hardness vs mineral crystallinity and collagen maturity. Each plot represents the mean of all data in a single specimen; bars show the standard error of the mean. Right: 3-dimensional scatter diagram of the left plots (mean values only). M, n = 8; C, n = 8.

mineral maturity (specifically, the apatitic-to-nonapatitic phosphate ratio) and a significant correlation of indentation modulus with the mineral-to-matrix ratio but not with either mineral maturity or collagen maturity. The MK-4–induced increase in mineral maturity rather than the increase in collagen maturity seems to be implicated in the increased hardness. That is, collagen maturity exerts a primary effect on the ultimate strength and toughness of bone rather than on its strength or stiffness because the collagen network is responsible for storing energy in the bone [42].

The effect of vitamin K on bone quality depends on the rat strain, dosage, and duration of administration; furthermore, vitamin K may have an age-dependent effect on the γ-carboxylation of OC [43]. It is unlikely that the present amount of MK-4 supplementation (22 mg d^{-1} kg^{-1} body weight) suffices for full effectiveness. Maximal benefits to bone quality during growth, including the promotion of cortical mineral accretion, might be achieved with a higher amount or a longer period of supplementation. Indeed, a recent study showed the beneficial effects of MK-4 in increasing femoral bone volume, width, and strength parameters in rats when it was supplemented in a larger amount (30-35 mg d^{-1} kg^{-1} body weight) over a longer period (3 months) starting at the age of 6 weeks [44].

The daily intake of vitamin K is 24 μg in 4-year-old British children [45], 51 μg in American children aged 2 to 8 years [46], and 279 μg in Japanese premenarche females aged 12 to 18 years who live in Tokyo, where fermented soybeans rich in MK-7 are consumed [47]. These vitamin K intakes seem to be insufficient for promoting bone health during childhood and adolescence, periods characterized by high bone metabolism [17,48,49]. Thus, similar to the situation in patients with high bone metabolism, daily supplementation of MK-4 may be effective for bone health during growth. In patients aged 3 to 18 years with classic galactosemia, a dose of 1 mg/d vitamin K_1 enhanced the γ-carboxylation of OC and played a positive role in the treatment of abnormal bone mineral content [50]. In patients with cystic fibrosis aged 6 to 17 years, a dose of 10 mg/d vitamin K_1 decreased Glu-OC levels even below those of healthy controls aged 8 to 17 years [51]. In the adult population of Japan, MK-4 is currently given at 45 mg/d for the treatment of postmenopausal osteoporosis or protection against fractures [52]. Meanwhile, another study showed that daily supplementation with 5 mg/d vitamin K_1 was protective against fractures in postmenopausal women with osteopenia [53]. These pharmacological doses are fairly low compared with the daily MK-4 doses according to body weight administered to rats in the present study; however, adverse effects, including weight gain and gastrointestinal complaints, were found in a small percentage of patients in a previous study [54]. In healthy Dutch children aged 6 to 10 years, Glu/Gla-OC dropped 33 % when they were supplemented with 45 μg/d MK-7, which is equivalent to 31 μg/d MK-4, for 8 weeks [14]. It is uncertain, however, whether this vitamin K supplementation is effective for bone properties. Additional studies should be designed to examine whether vitamin K doses in a more nutritional range promote bone strength during growth.

The Glu/Gla-OC ratio, which is independent of bone turnover, has been used as a sensitive marker for bone vitamin K status [15,55]. Vitamin K has protective effects against fractures in postmenopausal women, despite the lack of a significant change or the occurrence of only a modest increase in bone mineral density [52,56]. That is, vitamin K status is associated with better bone quality; and therefore, Glu/Gla-OC might be used as an indicator of bone quality in this population. In children, however, Glu/Gla-OC may not be exclusively indicative of bone quality because an association of vitamin K status with childhood bone mineral content has been observed [9].

Some limitations of this study should be noted. First, more Gla-OC will be bound to bone rather than circulating in the blood stream, thereby lowering serum Gla-OC. Thus, the Glu/Gla-OC ratio would underestimate the effect of vitamin K on the γ-carboxylation of OC. Second, the contact area (A_c in Eq. [2]) generated with the test load in nanoindentation was 10 μm^2 at most and much smaller than the area of 50 × 50 μm^2 from which FTIR spectra were collected. Consequently, it would be difficult to assess the correlations between mechanical and chemical properties, although 5 indents were included in the area of 50 × 50 μm^2 for FTIR-MS. Actually, there was no correlation between the mechanical indices averaged over 5 indents and chemical indices in each group (48 points) or in the 2 groups combined. A smaller measurement field of the FTIR-IR or a higher density of indents will be required to detect the correlations between mechanical and chemical properties [30,57]. Finally, we performed FTIR-MS and the nanoindentation test only at the cortical midlayers of the anterior and posterior cortices; consequently, the effect of MK-4 on the chemical and mechanical indices did not differ significantly between these measurement points. However, at other sites, such as the medial and lateral cortices or periosteal and endocortical layers, the mechanical milieu or rates of bone formation/resorption, which are influential in regulating bone tissue maturation, are different from those in the anterior and posterior cortical midlayers [58,59]. Thus, it remains possible that the effect of MK-4 on the intrinsic properties of bone tissue varies from site to site.

In conclusion, the beneficial effects of MK-4 supplementation on vitamin K status enhanced trabecular bone architecture and the maturation of cortical bone tissue in the growing rat tibia. Thus, MK-4 supplementation could be beneficial for enhancing bone quality and reducing fracture risk during growth spurts.

Funding

Part of this work was supported by 2 Grants-in-Aid for Scientific Research (19650116 and 21650112) from the Ministry of Education, Culture, Sports, Science, and Technology of Japan.

Acknowledgment

The authors are indebted to Eisai Pharmaceutical, Japan, for its donation of MK-4 (menatetrenone). The SR experiments were performed at SPring-8 with the approval of the Japan Synchrotron Radiation Research Institute (proposal no. 2007A1246/BL20B2).

Conflict of Interest

All authors of this manuscript certify that there is no conflict of interest with any financial and personal relationships with other people or organizations that could inappropriately influence this study.

REFERENCES

[1] Rauch F, Neu C, Manz F, et al. The development of metaphyseal cortex: implications for distal radius fractures during growth. J Bone Miner Res 2001;16:1547-55.
[2] Lyons RA, Sellstrom E, Delahunty AM, et al. Incidence and cause of fractures in European districts. Arch Dis Child 2000;82:452-5.
[3] Khosla S, Melton LJ, Dekutoski MB, et al. Incidence of childhood distal forearm fractures over 30 years: a population-based study. JAMA 2003;290:1479-85.
[4] Boot AM, de Ridder MA, van der Sluis IM, et al. Peak bone mineral density, lean body mass and fractures. Bone 2010;46: 336-41.
[5] Cooper C, Westlake S, Harvey N, et al. Review: developmental origins of osteoporotic fracture. Osteoporos Int 2006;17: 337-47.
[6] Goulding A, Jones IE, Taylor RW, et al. More broken bones: a 4-year double cohort study of young girls with and without distal forearm fractures. J Bone Miner Res 2000;15:2011-8.
[7] Hernandez CJ, Beaupré GS, Carter DR. A theoretical analysis of the relative influences of peak BMD, age-related bone loss and menopause on the development of osteoporosis. Osteoporos Int 2003;14:843-7.
[8] Rizzoli R, Bianchi ML, Garabédian M, et al. Maximizing bone mineral mass gain during growth for the prevention of fractures in the adolescents and the elderly. Bone 2010;46:294-305.
[9] van Summeren MJ, van Coeverden SC, Schurgers LJ, et al. Vitamin K status is associated with childhood bone mineral content. Br J Nutr 2008;100:852-8.
[10] Hauschka PV, Lian JB, Cole DE, et al. Osteocalcin and matrix Gla protein: vitamin K–dependent proteins in bone. Physiol Rev 1989;69:990-1047.
[11] Ichikawa T, Horie-Inoue K, Ikeda K, et al. Steroid and xenobiotic receptor SXR mediates vitamin K2–activated transcription of extracellular matrix–related genes and collagen accumulation in osteoblastic cells. J Biol Chem 2006;281:16927-34.
[12] Igarashi M, Yogiashi Y, Mihara M, et al. Vitamin K induces osteoblast differentiation through pregnane X receptor–mediated transcriptional control of the Msx2 gene. Mol Cell Biol 2007;27:7947-54.
[13] Yamaguchi M, Ma ZJ. Inhibitory effect of menaquinone-7 (vitamin K2) on osteoclast-like cell formation and osteoclastic bone resorption in rat bone tissues in vitro. Mol Cell Biochem 2001;228:39-47.
[14] van Summeren MJ, Braam LA, Lilien MR, et al. The effect of menaquinone-7 (vitamin K2) supplementation on osteocalcin carboxylation in healthy prepubertal children. Br J Nutr 2009;102:1171-8.
[15] Vermeer C, Shearer MJ, Zittermann A, et al. Beyond deficiency: potential benefits of increased intakes of vitamin K for bone and vascular health. Eur J Nutr 2004;43:325-35.
[16] Szulc P, Seeman E, Delmas PD. Biochemical measurements of bone turnover in children and adolescents. Osteoporos Int 2000;11:281-94.
[17] van Summeren M, Braam L, Noirt F, et al. Pronounced elevation of undercarboxylated osteocalcin in healthy children. Pediatr Res 2007;61:366-70.
[18] Nakagawa K, Hirota Y, Sawada N, et al. Identification of UBIAD1 as a novel human menaquinone-4 biosynthetic enzyme. Nature 2010;468:117-21.
[19] Boskey A, Pleshko Camacho N. FT-IR imaging of native and tissue-engineered bone and cartilage. Biomaterials 2007;28: 2465-78.
[20] Paschalis EP. Fourier transform infrared analysis and bone. Osteoporos Int 2009;20:1043-7.
[21] Hengsberger S, Ammann P, Legros B, et al. Intrinsic bone tissue properties in adult rat vertebrae: modulation by dietary protein. Bone 2005;36:134-41.
[22] Lewis G, Nyman JS. The use of nanoindentation for characterizing the properties of mineralized hard tissues: state-of-the art review. J Biomed Mater Res B Appl Biomater 2008;87: 286-301.
[23] Müller R, Rüegsegger P. Micro-tomographic imaging for the nondestructive evaluation of trabecular bone architecture. Stud Health Technol Inform 1997;40:61-79.
[24] Martín-Badosa E, Amblard D, Nuzzo S, et al. Excised bone structures in mice: imaging at three-dimensional synchrotron radiation micro CT. Radiology 2003;229:921-8.
[25] Matsumoto T, Yoshino M, Asano T, et al. Monochromatic synchrotron radiation μCT reveals disuse-mediated canal network rarefaction in cortical bone of growing rat tibiae. J Appl Physiol 2006;100:274-80.
[26] Matsumoto T, Ando N, Tomii T, et al. Three-dimensional cortical bone microstructure in rat model of hypoxia-induced growth retardation. Calcif Tissue Int 2011;81:54-62.
[27] Otsu N. Threshold selection method from gray-level histograms. IEEE Trans Syst Man Cybern 1979;9:62-6.
[28] Hildebrand T, Ruegsegger P. A new method for the model-independent assessment of thickness in three-dimensional images. J Microsc 1997;185:67-75.
[29] Hengsberger S, Kulik A, Zysset P. Nanoindentation discriminates the elastic properties of individual human bone lamellae under dry and physiological conditions. Bone 2002;30:178-84.
[30] Busa B, Miller LM, Rubin CT, et al. Rapid establishment of chemical and mechanical properties during lamellar bone formation. Calcif Tissue Int 2005;77:386-94.

[31] Dong A, Huang P, Caughey WS. Protein secondary structures in water from second-derivative amide I infrared spectra. Biochemistry 1990;29:3303-8.
[32] Gadaleta SJ, Paschalis EP, Betts F, et al. Fourier transform infrared spectroscopy of the solution-mediated conversion of amorphous calcium phosphate to hydroxyapatite: new correlations between x-ray diffraction and infrared data. Calcif Tissue Int 1996;58:9-16.
[33] Silva MJ, Brodt MD, Fan Z, et al. Nanoindentation and whole-bone bending estimates of material properties in bones from the senescence accelerated mouse SAMP6. J Biomech 2004;37: 1639-46.
[34] Oliver WC, Pharr GM. Measurement of hardness and elastic modulus by instrumented indentation: advances in understanding and refinements to methodology. J Mater Res 2004;19:3-20.
[35] Onodera K, Takahashi A, Sakurada S, et al. Effects of phenytoin and/or vitamin K2 (menatetrenone) on bone mineral density in the tibiae of growing rats. Life Sci 2002;70: 1533-42.
[36] Iwamoto J, Matsumoto H, Takeda T, et al. Effects of vitamin K2 and risedronate on bone formation and resorption, osteocyte lacunar system, and porosity in the cortical bone of glucocorticoid-treated rats. Calcif Tissue Int 2008;83:121-8.
[37] Iwasaki Y, Yamato H, Murayama H, et al. Maintenance of trabecular structure and bone volume by vitamin K2 in mature rats with long-term tail suspension. J Bone Miner Metab 2002;20:216-22.
[38] Kobayashi M, Hara K, Akiyama Y. Infrared analysis of bones in magnesium-deficient rats treated with vitamin K2. J Bone Miner Metab 2007;25:12-8.
[39] Parfitt AM. The physiologic and clinical significance of bone histomorphometric data. In: Recker R, editor. Bone histomorphometry. Techniques and interpretations. Boca Raton: CRC Press; 1983. p. 143-223.
[40] Matsumoto T, Yoshino M, Uesugi K, et al. Biphasic change and disuse-mediated regression of canal network structure in cortical bone of growing rats. Bone 2007;41:239-46.
[41] Farlay D, Panczer G, Rey C, et al. Mineral maturity and crystallinity index are distinct characteristics of bone mineral. J Bone Miner Metab 2010;28:433-45.
[42] Burr DB. The contribution of the organic matrix to bone's material properties. Bone 2002;31:8-11.
[43] Tsugawa N, Shiraki M, Suhara Y, et al. Vitamin K status of healthy Japanese women: age-related vitamin K requirement for γ-carboxylation of osteocalcin. Am J Clin Nutr 2006;83: 380-6.
[44] Sogabe N, Maruyama R, Baba O, et al. Effects of long-term vitamin K1 (phylloquinone) or vitamin K2 (menaquinone-4) supplementation on body composition and serum parameters in rats. Bone 2011;48:1036-42.
[45] Prynne CJ, Thane CW, Prentice A, et al. Intake and sources of phylloquinone (vitamin K1) in 4-year-old British children: comparison between 1950 and the 1990s. Public Health Nutr 2005;8:171-80.
[46] Bounds W, Skinner J, Carruth BR, et al. The relationship of dietary and lifestyle factors to bone mineral indexes in children. J Am Diet Assoc 2005;105:735-41.
[47] Kuroda T, Onoe Y, Miyabara Y, et al. Influence of maternal genetic and lifestyle factors on bone mineral density in adolescent daughters: a cohort study in 387 Japanese daughter-mother pairs. J Bone Miner Metab 2009;27:379-85.
[48] Collins A, Cashman KD, Kiely M. Vitamin K1 intake and status in Irish adolescent girls. Int J Vitam Nutr Res 2006;76:385-90.
[49] O'Connor E, Mølgaard C, Michaelsen KF, et al. Serum percentage undercarboxylated osteocalcin, a sensitive measure of vitamin K status, and its relationship to bone health indices in Danish girls. Br J Nutr 2007;97:661-6.
[50] Panis B, Vermeer C, van Kroonenburgh MJ, et al. Effect of calcium, vitamins K1 and D3 on bone in galactosemia. Bone 2006;39:1123-9.
[51] Nicolaidou P, Stavrinadis I, Loukou I, et al. The effect of vitamin K supplementation on biochemical markers of bone formation in children and adolescents with cystic fibrosis. Eur J Pediatr 2006;165:540-5.
[52] Iwamoto J, Satob Y, Takeda T, et al. High-dose vitamin K supplementation reduces fracture incidence in postmenopausal women: a review of the literature. Nutr Res 2009;29:221-8.
[53] Cheung AM, Tile L, Lee Y, et al. Vitamin K supplementation in postmenopausal women with osteopenia (ECKO trial): a randomized controlled trial. PLoS Med 2008;5:1-12.
[54] Knapen MH, Schurgers LJ, Vermeer C. Vitamin K2 supplementation improves hip bone geometry and bone strength indices in postmenopausal women. Osteoporos Int 2007;18: 963-72.
[55] Sokoll LJ, Sadowski JA. Comparison of biochemical indexes for assessing vitamin K nutritional status in a healthy adult population. Am J Clin Nutr 1996;63:566-73.
[56] Tsugawa N, Shiraki M, Suhara Y, et al. Low plasma phylloquinone concentration is associated with high incidence of vertebral fracture in Japanese women. J Bone Miner Metab 2008;26:79-85.
[57] Donnelly E, Boskey AL, Baker SP, et al. Effects of tissue age on bone tissue material composition and nanomechanical properties in the rat cortex. J Biomed Mater Res A 2010;92: 1048-56.
[58] Goodwin KJ, Sharkey NA. Material properties of interstitial lamellae reflect local strain environments. J Orthop Res 2002;20:600-6.
[59] Sontag W. Quantitative measurements of periosteal and cortical-endosteal bone formation and resorption in the midshaft of male rat femur. Bone 1986;7:63-70.